INT J APPL ELECTR PHYS & ROBOT, Vol. 1 No. 1 July (2013) pp. 18–23
ISSN: 2203-0069
International Journal of Applied Electronics in Physics & Robotics

Research Article

Evaluation of Wavelet–Functions for Broken Rotor Bar Detection of Induction Machine Using Coefficient–Related Features

Mohammad Rezazadeh Mehrjou[1,*], Norman Mariun[1], Mahdi Karami[1], Norhisam Misron[1], Saman Toosi[1], Mohammad Reza Zare[1,2]

(1) Department of Electrical and Electronic Engineering, University Putra Malaysia, Selangor, Malaysia.
(2) Department of Electrical and Electronic Engineering, Islamic Azad University Majlesi Branch, Majlesi, Iran.

doi:10.7575/aiac.ijaepr.v.1n.1p.18

Article history:
Received 16 July 2013
Reviewed 20 July 2013
Revised 23 July 2013
Accepted 24 July 2013
Published 26 July 2013

Abstract. *Early fault detection of the induction machine is necessary in order to guarantee its stable and high performance. To evaluate the motor's health and detect existence of any failure in it, any motor parameter is first measured using condition monitoring techniques. The raw signal acquired is then interpret applying signal processing and data analysis procedures. Wavelet analysis of the motor current has been considered as an effective fault detection method. However, there are different types of the wavelet function that can be used for signal decomposition. This paper intends to investigate the ability of different types of wavelet functions for early broken rotor bar detection. Different harmonic components introduced by this fault such as maximum wavelet coefficient, left and right gradients of the maximum coefficient, were extracted and used as a characteristic signature for fault detection. The results indicate that the reliability of the fault detection depends on the type of wavelet function applied for decomposition of the signal.*

Keywords: induction machine, fault, broken rotor bar, current signature, signal processing, wavelet analysis.

1 Introduction

A wide variety of types for squirrel cage induction machines (SCIMs) facilitate industrial tasks and productions. In industrial area, SCIMs are subjected to electrical, mechanical and environmental stresses that cause broken rotor bar (BRB) occurs, although SCIMs have rugged structure. The presence of BRB brings about secondary malfunctions that reduces the efficiency of the motor and hence increase the operational cost[1]. Accordingly, early detection of rotor failures, specially BRB, is crucial[2]. Any problem or irregularity in the machine can be detected at an early stage by applying a suitable condition monitoring accompanied with an effective signal processing method. Several condition monitoring techniques for SCIMs fault detection have been reported and developed[2,3]. Among various condition monitoring techniques, motor current signature analysis has been widely employed for BRB detection[4–7]. However, the fault detection will fail if an effective signal processing method is not applied. A raw signal measured by a suitable sensor goes through a signal processing to generate parametric features associated with the fault under observation. These features, generally known as "fault signature", are sensitive to the presence of the failure in motor. Fundamentally, the main aspects for the accurate detection and extraction of these features are based on signal processing. The technique applied to the signal must have high sensitivity to the features. It must be able to determinate the relationship between the fault signature and its severity as well[8].

Recently, wavelet analysis that allows simultaneous time and frequency decomposition of a signal has drawn the great attention. Nevertheless, the results of analysis depend on the type of wavelet function applied for signal decomposition. Besides that, various fault signatures can be extracted by applying wavelet decomposition to the raw current signal. The objective of this research is to examine using different types of wavelet functions in wavelet decomposition of the stator current signal. A variety of fault features are extracted and investigated for early detection of BRB.

2 Motor Current Signature Analysis

The current drawn by a healthy induction motor contains a single component in the spectrum of stator current. Existence of any asymmetry in induction motor generates extra component in the spectrum which is corresponding to the fault. For example, when a rotor breaks, current can not flow through it, and thus no magnetic flux is generated around that bar. Therefore an asymmetry is generated in the magnetic field of rotor by producing a non–zero backward rotating field. This phenomenon can be observed in the stator spectrum at the

*Corresponding author: M. R. Mehrjou
☎: +6 (0)17 201 9766
✉: mehrjou.mo@gmail.com

frequency corresponding to twice of the slip frequency, as[9,10].

$$f_b = (1 \pm 2ks) f_s \tag{1}$$

where f_b is the frequency of the current related to BRB and/or end–ring fault; s is the slip; k is a constant value and f is the supply frequency.

Frequency domain analysis, based on Fourier transform, is the most common signal processing technique used for f_b extraction. However, there are some inconsistencies regarding the ability of Fourier based analysis for early fault detection[11,12], and therefore advanced signal processing techniques were proposed for more accurate and reliable fault detection. These techniques, such as wavelet transform analysis, are based on simultaneous time and frequency analysis of the signal. Wavelet transform analysis is classified to continuous and discrete. Continuous wavelet transform (CWT) is a sum over all time of the signal multiplied by scaled, shifted versions of the wavelet function. In this procedure, the wavelet coefficient at all scales is calculated that produces a lot of data and obviously it takes a long time[13]. Discrete wavelet transform analyses the signals with a smaller set of scales and specific number of translations at each scale. Mallat[14] introduced a practical version of discrete wavelet transform, called wavelet multi–resolution analysis. This algorithm is based on the fact that, one signal is decomposed into series of small waves belonging to a wavelet family. A discrete signal $f[t]$ could be decomposed as

$$f[t] = \sum_k A_{m_0,n}\phi_{m_0,n}[t] + \sum_{m=m_0}^{m-1}\sum_n D_{m,n}\psi_{m,n}[t] \tag{2}$$

where ϕ is the scaling functions, deduced by father wavelet and ψ is the wavelet functions, deduced by mother wavelet, A is approximate coefficients and D is detail coefficients. The multi–resolution analysis commonly uses discrete dyadic wavelet, in which scales and positions are based on powers of two. In this approach, the scaling function is represented by the following mathematical expression:

$$\phi_{m_o,n}[t] = 2^{\frac{m_0}{2}}\phi(2^{m_0}t - n) \tag{3}$$

i.e. $\phi_{m_0,n}$ is the scaling function at a scale of 2^{m_0} shifted by n. Wavelet function is also defined as

$$\psi_{m,n}[t] = 2^{\frac{m}{2}}\psi(2^m t - n) \tag{4}$$

i.e. $\psi_{m,n}$ is the mother wavelet at a scale of 2^m shifted by n.

Generally, approximate coefficients $A_{m_0,n}$ are obtained through the inner product of the original signal and the scaling function.

$$A_{m_0,n} = \int_{-\infty}^{\infty} f(t)\phi_{m_0,n}(t)dt \tag{5}$$

The approximate coefficients decomposed from a discretized signal can be expressed as

$$\begin{aligned} A_{m+1,n} &= \sum_{n=0}^{N} A_{m,n}\int \phi_{m,n}(t)\phi_{m+1,n}(t)dt \\ &= \sum A_{m,n}g[n] \end{aligned} \tag{6}$$

In dyadic approach, the approximation coefficients $A_{m_0,n}$ are at a scale of 2^{m_0}. The filter, $g[n]$, is a low–pass filter.

Similarly the detail coefficients $D_{m,n}$ can be generally obtained through the inner product of the signal and the complex conjugate of the wavelet function.

$$D_{m,n} = \int_{-\infty}^{\infty} f(t)\psi^*_{m,n}(t)dt \tag{7}$$

The detail coefficients decomposed from a discretized signal can be expressed as

$$\begin{aligned} D_{m+1,n} &= \sum_{n=0}^{N} A_{m,n}\int \phi_{m,n}(t)\psi_{m+1,n}(t)dt \\ &= \sum_n A_{m,n}h[n] \end{aligned} \tag{8}$$

$D_{m,n}$ are the detail coefficients at a scale of 2^{m_0}. The filter, $h[n]$ is a high–pass filter. The multi–resolution analysis utilizes discrete dyadic wavelet and extract the approximations of the original signal at different levels of resolution. An approximation is a low resolution representation of the original signal. The approximation at a resolution 2^{-m} can be split into an approximation at a coarser resolution $2^{-(m+1)}$ and the detail. The detail represents the high frequency contents of the signal. The approximations and details can be determined using low and high pass filters. In the multi–resolution analysis, the approximations are split successively, while the details are never analysed further. The decomposition process can be iterated, with successive approximations being decomposed in turn, hence one signal is broken down into many lower resolution components. This process is called the wavelet decomposition tree as shown in Fig. 1[15].

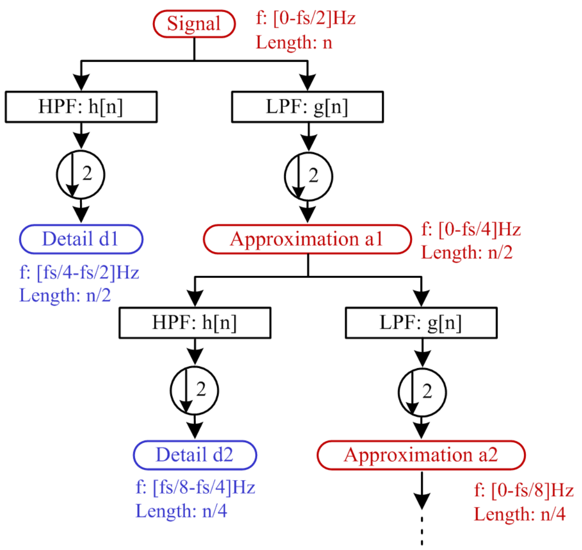

Fig. 1. Dyadic Wavelet Decomposition Algorithm

Wavelet transform analysis though is proposed as one of the best technique for fault detection, it has some limitation that should be taken into account. For instance, the type of wavelet function determines the result of signal decomposition and various features can be extracted from decomposed signal. Therefore, a comparative study that concentrates on the outcomes of different wavelet functions for early fault detection is essential. This study intends to investigate the effects of the wavelet function and characteristic feature for early BRB detection using wavelet analysis of stator current spectrum.

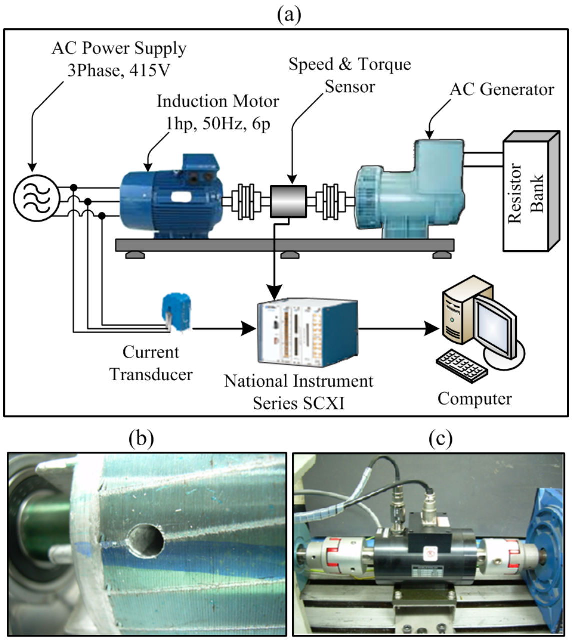

Fig. 2. a) Experimental Setup, b) One broken rotor bar, c) Torque and speed sensor

3 Case study

To examine the reliability of wavelet transform analysis for early detection of BRB, two motors, one motor with no broken bar and the other with one broken bar, were observed under different levels of load (35%, 50% and 80% full load). The induction machine was coupled to an generator acting as a load. Experimental data including torque, speedcurrent and was acquired through the appropriate sensors. Fig. 2 demonstrates the experimental setup used in this study. The main characteristics of the test motor was star connection, power was 750 W, voltage was 415 V, six poles, primary current was 2.2 A, speed was 1000 rpm and the number of 28 rotor bars.

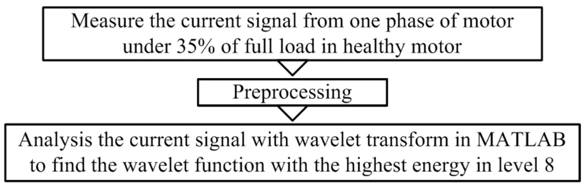

Fig. 3. Steps to find the suitable Wavelet function

A bar breakage in the rotor was forced by drilling it artificially in the laboratory. For the test motor, current signal was measured using a board comprised of Hall Effect current sensors, LEM–LA–25P. Data was acquired using a system bought from National Instrument company (SCXI 1125&1140 and PCI 6052E) and then was sent to a PC for analysis in MATLAB environment. The stator current was sampled at 20 kHz and the capturing time was 0.2 s. Motor speed and torque were also observed to ensure that the test motor works in a similar condition for each test.

Before data analysis, the raw current signal was re–sampled by synchronizing the starting origin with phase 0. This preprocessing of the raw current signal is critical since the unsynchronized current phase will give inaccurate detection results[12,16]. The total re–sampled cycles of the signals were five cycles, *i.e.* about 2400 sampled data were used for analysis.

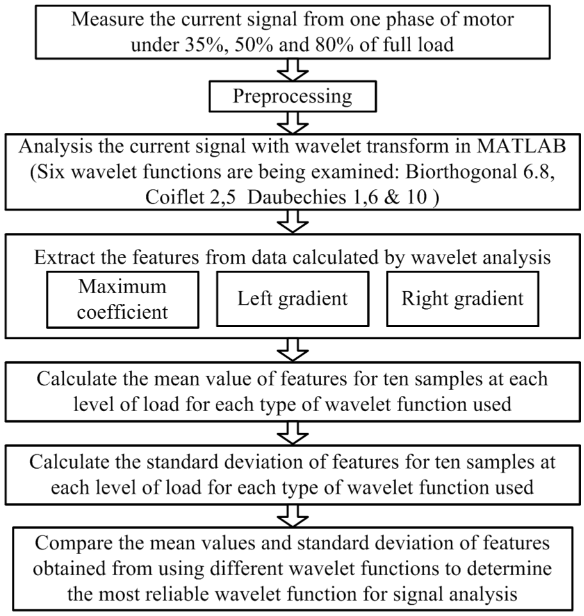

Fig. 4. The flow chart diagram applied in this study for broken rotor bar detection

Discrete wavelet transform provides a set of decomposed signals in independent frequency bands that depends upon the level of decomposition. Therefore, to obtain a signal that encompasses frequencies of interest, the level of decomposition first was determined. The stator current signal was decomposed at 11 levels that the detail of the 8^{th} level was used for analysis, since it encompasses the frequency bandwidth between 39.06 and 78.12 Hz (fundamental frequency is 50Hz). Fault characteristic features were extracted from the signal corresponds to detail of the 8th decomposition level.

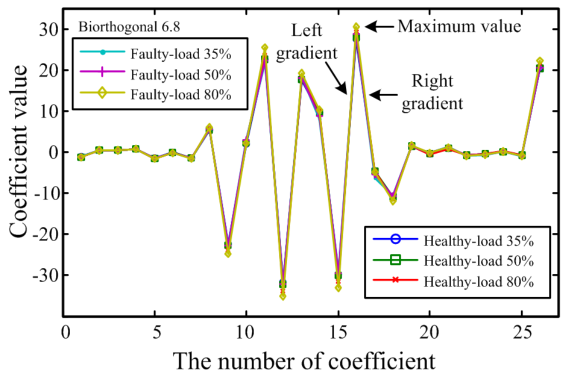

Fig. 5. Wavelet coefficients of the 8th detail for healthy and faulty motors using Biorthogonal 6.8 at different levels of loads

In the following step, all wavelet functions provided by wavelet tool box in MATLAB ware examined to find the suitable Wavelet function, as depicted in Fig. 3. The wavelet functions that generate a decomposed signal with higher energy value in determined level of decomposition were selected for the fault detection.

Three features, including the maximum coefficient value and its gradients, were extracted from wavelet decomposition of current signal using the six wavelet functions selected in the previous step. Each test was repeated 10 times and the average value of the features were calculated and used for further investigation. Fig. 4 depicts the procedure used for wavelet analysis of current signal.

doi:10.7575/aiac.ijaepr.v.1n.1p.18

Table 1. Characteristic features of the 8th detail decomposition for healthy motor under different levels of load when various types of wavelet function were used

Feature	Load (%)	Bior 6.8	Coiflet 2	Coiflet 5	Daub 1	Daub 6	Daub 10
Left gradient	35	57.23	55.13	**30.55**	40.45	**38.00**	53.81
	50	57.99	55.84	**30.39**	41.15	**38.16**	**54.11**
	80	60.94	58.67	31.72	43.42	40.16	56.84
Peak value	35	27.56	26.89	**26.92**	23.03	**29.25**	**32.61**
	50	28.10	27.40	**27.09**	23.43	**29.37**	**32.91**
	80	29.51	28.77	28.43	24.62	30.89	34.49
Right gradient	35	-32.25	-33.03	**-58.92**	-34.26	**-57.15**	-52.25
	50	-32.69	-33.46	**-59.47**	-34.97	-57.64	-53.06
	80	-34.07	-34.88	-62.48	-36.74	-60.47	-55.61

Table 2. Characteristic features of the 8th detail decomposition for faulty motor under different levels of load when various types of wavelet function were used

Feature	Load (%)	Bior 6.8	Coiflet 2	Coiflet 5	Daub 1	Daub 6	Daub 10
Left gradient	35	57.68	55.42	**28.63**	40.61	**36.38**	52.58
	50	58.34	56.18	**29.54**	41.26	**37.57**	**53.57**
	80	63.59	61.15	34.53	45.22	42.75	59.83
Peak value	35	28.75	27.89	**26.31**	23.30	**28.64**	**32.45**
	50	28.86	28.13	**26.89**	23.57	**29.15**	**32.77**
	80	30.66	29.88	30.38	25.64	32.34	36.31
Right gradient	35	-34.23	-34.81	**-58.68**	-36.01	**-57.13**	-53.79
	50	-34.98	-34.93	**-59.44**	-36.05	-57.68	-53.92
	80	-35.44	-36.25	-65.73	-38.25	-63.52	-58.56

As an example, Fig. 5 illustrates the wavelet coefficients of the 8^{th} detail for healthy and faulty motor using Biorthogonal 6.8 at different levels of load. Wavelet analysis using Biorthogonal 6.8 generates a set of 26 coefficients for each case. Fig. 5 shows that for all cases, the 16^{th} coefficient has the maximum value. Therefore, the 16^{th} coefficient and its gradients (left and right gradient) were selected as features for BRB detection. The left gradient corresponds to the slope of line drawn from 16^{th} coefficient to the previous one (15^{th}). The right gradient is the line slope between maximum coefficient (16^{th} coefficient) and the 17^{th} coefficient.

In a similar way, other types of wavelet function such as Coiflet 2, Coiflet 5, Daubechies 1, Daubechies 6 and Daubechies 10 were used for signal analysis. The number of wavelet coefficients depends upon the type of wavelet function used for analysis of the signal. The maximum value for coefficient and its gradients were used as signature for BRB detection. Fig. 6 illustrates the zoom-in demonstration around the maximum coefficient determined for each wavelet function. Besides maximum coefficient and its gradients, the energy value of the decomposed signal at 8^{th} detail was determined and considered as a fault characteristic feature. Table 1 and Table 2 present the mean values for the characteristic features of the 8^{th} detail decomposition for healthy and faulty machines under different levels of load when various types of wavelet function were applied for signal decomposition.

It has been proven in case of fault presence in the motor, the fault signatures have higher values than the one for healthy condition[17,18]. However, the data presented in Table 1 and Table 2 indicate some inconsistencies. For instance, that, when Coiflet 5, Daubechies 6 and Daubechies 10 were used, values for left gradient and maximum coefficient for faulty motor were smaller than healthy motor. The same observation was made for the right gradient when Coiflet 5 and Daubechies 6 were used as a wavelet function. No such inconsistencies were observed when Biorthogonal 6.8, Coiflet 2 and Daubechies 1 were applied for wavelet decomposition of the signal. These observations express that not only the type of wavelet function used for signal analysis influence the result but also the characteristic feature needs to be taken into account.

Table 3. Statistical parameters computed for characteristic features obtained from wavelet analysis of the current signal using Biorthogonal 6.8 and Daubechies 1

			Healthy				Faulty (one BRB)			
			Biorthogonal 6.8		Daubechies 1		Biorthogonal 6.8		Daubechies 1	
Feature	Torque (N.m)	Load (%)	Mean	STD	Mean	STD	Mean	STD	Mean	STD
Left gradient	2.70	35	57.23	0.06	40.45	**0.06**	57.68	0.14	40.61	0.29
	4.00	50	57.99	**0.09**	41.15	0.13	58.34	0.31	41.26	**0.19**
	6.25	80	60.94	0.06	43.42	**0.06**	63.59	0.41	45.22	**0.08**
Peak value	2.70	35	27.56	0.12	23.03	**0.04**	28.75	0.24	23.30	**0.17**
	4.00	50	28.10	0.28	23.43	**0.06**	28.86	0.30	23.57	**0.14**
	6.25	80	29.51	0.13	24.62	**0.04**	30.66	0.45	25.64	**0.05**
Right gradient	2.70	35	-32.25	0.34	-34.26	**0.15**	-34.23	0.81	-36.01	**0.46**
	4.00	50	-32.69	0.74	-34.97	**0.30**	-34.98	0.85	-36.05	**0.50**
	6.25	80	-34.07	0.30	-36.74	**0.12**	-35.44	0.80	-38.25	**0.63**

Since just three wavelet functions, Biorthogonal 6.8, Coiflet 2 and Daubechies 1, showed reliable information, these three were further investigated. The standard deviations of all features for these three wavelet functions were computed as presented in Table 3. Comparatively, Daubechies 1 had smaller standard deviation that indicates the sampled data had smaller dispersion from the average. Therefore, the characteristic features obtained from decomposition of current signal using Daubechies 1 were more reliable to be used for incipient fault detection in SCIM than Biorthogonal 6.8 and Coiflet 2. In this study, it has been proven that there is a significant difference in ability of wavelet functions for accurate signal analysis and interpretation. Therefore, the arbitrary selection of wavelet function for wavelet analysis of signal cannot provide reliable information for fault detection in motor. Moreover, it is recommended that different char-

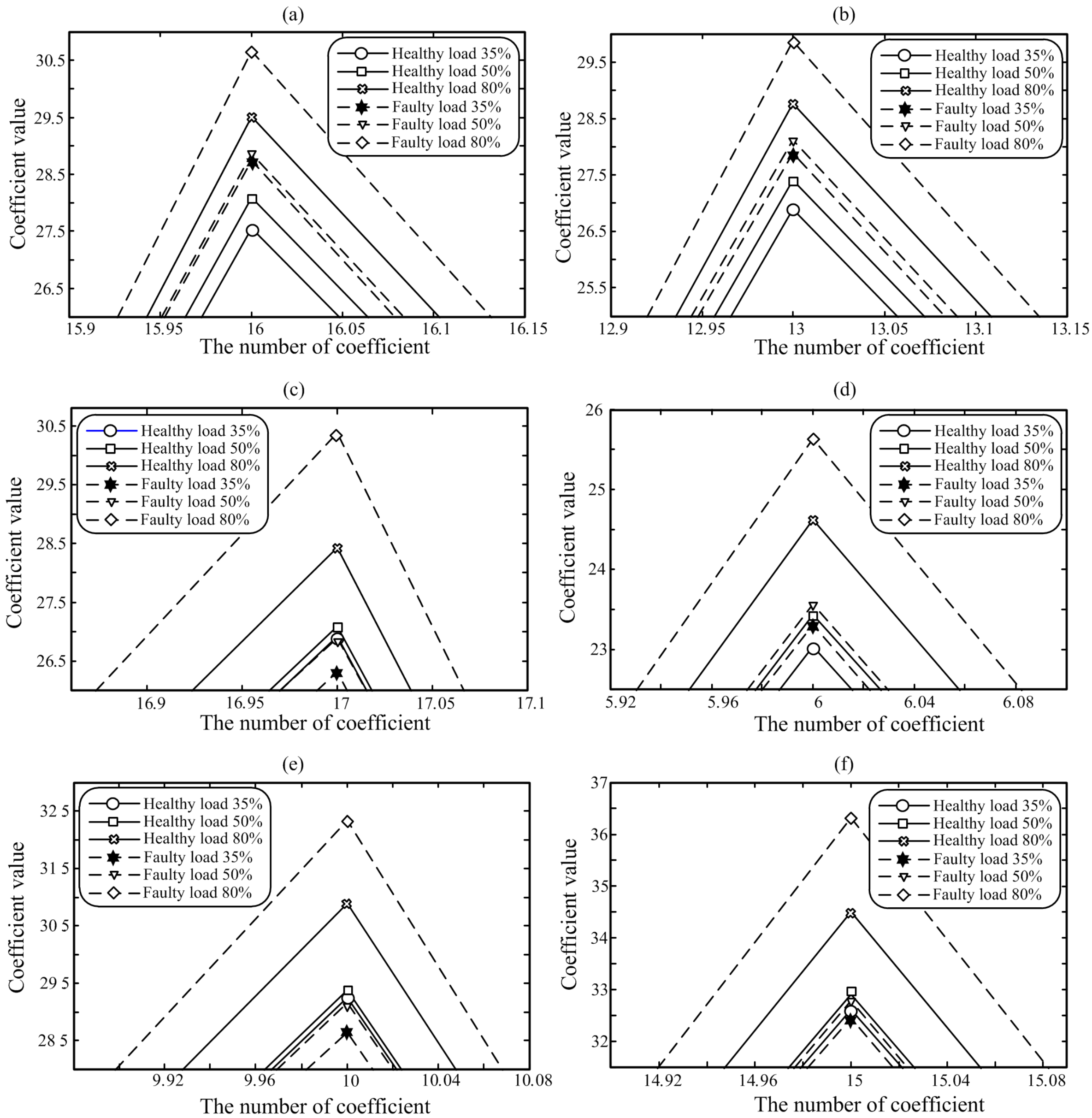

Fig. 6. The zoom-in graph around the maximum wavelet coefficient for healthy and faulty motors using a) Biorthogonal 6.8, b) Coiflet 2, c) Coiflet 5, d) Daubechies 1, e) Daubechies 6, f) Daubechies 10

acteristic features to be selected and observed as the accuracy of the monitoring will be enhanced.

4 Conclusion

In this study, different types of wavelet functions were examined for early detection of BRB in SCIM. The functions were applied to decompose the current signal, and compared in screening the features related to the present fault. The characteristic features observed were the maximum wavelet coefficients, left and right gradients of the maximum coefficient. This study proved that the types of wavelet function used for signal analysis influence the reliability of the diagnostic method. Among different wavelet functions examined in this research for current signal decomposition, Daubechies 1 provided much more reliable information for early detection of BRB. An increase in all characteristics features were observed for faulty motor compared to the healthy motor that worked under similar level of the load. Besides that, observing different characteristic features enhances the accuracy and reliability of the fault detection.

Acknowledgement

The authors gratefully acknowledge Universiti Putra Malaysia for granting the Research University Grant for conducting this work.

REFERENCES

[1] I. Culbert and W. Rhodes, “Using current signature analysis technology to reliably detect cage winding defects in squirrel cage induction motors,” in *Petroleum and Chemical Industry Conference, 2005. Industry Applications Society 52nd Annual*. IEEE, 2005, pp. 95–101.

[2] P. Zhang, Y. Du, T. G. Habetler, and B. Lu, “A survey of condition monitoring and protection methods for medium-voltage induction motors,” *Industry Applications, IEEE Transactions on*, vol. 47, no. 1, pp. 34–46, 2011.

[3] M. R. Mehrjou, N. Mariun, M. Hamiruce Marhaban, and N. Misron, “Rotor fault condition monitoring techniques for squirrel-cage induction machine–A review,” *Mechanical Systems and Signal Processing*, vol. 25, no. 8, pp. 2827–2848, 2011.

[4] L. Saidi, F. Fnaiech, H. Henao, G. Capolino, and G. Cirrinione, “Diagnosis of broken-bars fault in induction ma-

chines using higher order spectral analysis," *ISA transactions*, 2012.

[5] G. Didier, E. Ternisien, O. Caspary, and H. Razik, "A new approach to detect broken rotor bars in induction machines by current spectrum analysis," *Mechanical Systems and Signal Processing*, vol. 21, no. 2, pp. 1127–1142, 2007.

[6] F. Gu, Y. Shao, N. Hu, A. Naid, and A. Ball, "Electrical motor current signal analysis using a modified bispectrum for fault diagnosis of downstream mechanical equipment," *Mechanical Systems and Signal Processing*, vol. 25, no. 1, pp. 360–372, 2011.

[7] M. R. Mehrjou, N. Mariun, M. H. Marhaban, and N. Misron, "Evaluation of fourier and wavelet analysis for efficient recognition of broken rotor bar in squirrel-cage induction machine," in *Power and Energy (PECon), 2010 IEEE International Conference on*. IEEE, 2010, pp. 740–743.

[8] F. Filippetti, G. Franceschini, and C. Tassoni, "Neural networks aided on-line diagnostics of induction motor rotor faults," *Industry Applications, IEEE Transactions on*, vol. 31, no. 4, pp. 892–899, 1995.

[9] G. Kliman, R. Koegl, J. Stein, R. Endicott, and M. Madden, "Noninvasive detection of broken rotor bars in operating induction motors," *Energy Conversion, IEEE Transactions on*, vol. 3, no. 4, pp. 873–879, 1988.

[10] N. M. Elkasabgy, A. R. Eastham, and G. E. Dawson, "Detection of broken bars in the cage rotor on an induction machine," *Industry Applications, IEEE Transactions on*, vol. 28, no. 1, pp. 165–171, 1992.

[11] J. A. Antonino-Daviu, M. Riera-Guasp, J. R. Folch, and M. P. M. Palomares, "Validation of a new method for the diagnosis of rotor bar failures via wavelet transform in industrial induction machines," *Industry Applications, IEEE Transactions on*, vol. 42, no. 4, pp. 990–996, 2006.

[12] S.-H. Lee, S.-P. Cheon, Y. Kim, and S. Kim, "Fourier and wavelet transformations for the fault detection of induction motor with stator current," in *Computational Intelligence*. Springer, 2006, pp. 557–569.

[13] G. Niu, A. Widodo, J.-D. Son, B.-S. Yang, D.-H. Hwang, and D.-S. Kang, "Decision-level fusion based on wavelet decomposition for induction motor fault diagnosis using transient current signal," *Expert Systems with Applications*, vol. 35, no. 3, pp. 918–928, 2008.

[14] S. G. Mallat, "A theory for multiresolution signal decomposition: the wavelet representation," *Pattern Analysis and Machine Intelligence, IEEE Transactions on*, vol. 11, no. 7, pp. 674–693, 1989.

[15] R. Polikar, L. Udpa, S. S. Udpa, and T. Taylor, "Frequency invariant classification of ultrasonic weld inspection signals," *Ultrasonics, Ferroelectrics and Frequency Control, IEEE Transactions on*, vol. 45, no. 3, pp. 614–625, 1998.

[16] H. Bae, Y.-T. Kim, S.-H. Lee, S. Kim, and M. H. Lee, "Fault diagnostic of induction motors for equipment reliability and health maintenance based upon fourier and wavelet analysis," *Artificial Life and Robotics*, vol. 9, no. 3, pp. 112–116, 2005.

[17] K. Abbaszadeh, J. Milimonfared, M. Haji, and H. Toliyat, "Broken bar detection in induction motor via wavelet transformation," in *Industrial Electronics Society, 2001. IECON'01. The 27th Annual Conference of the IEEE*, vol. 1. IEEE, 2001, pp. 95–99.

[18] S.-h. Lee, J.-i. Song *et al.*, "Fourier and wavelet transformations application to fault detection of induction motor with stator current," *Journal of Central South University of Technology*, vol. 17, no. 1, pp. 93–101, 2010.